Int J Thermophys (2017) 38:49
DOI 10.1007/s10765-017-2183-0

TEMPMEKO 2016

Thermodynamic Temperature Measurement to the Indium Point Based on Radiance Comparison

Y. Yamaguchi[1] · **Y. Yamada**[1]

Received: 30 August 2016 / Accepted: 24 January 2017 / Published online: 13 February 2017

Abstract A multi-national project (the EMRP InK project) was completed recently, which successfully determined the thermodynamic temperatures of several of the high-temperature fixed points above the copper point. The National Metrology Institute of Japan contributed to this project with its newly established absolute spectral radiance calibration capability. In the current study, we have extended the range of thermodynamic temperature measurement to below the copper point and measured the thermodynamic temperatures of the indium point ($T_{90} = 429.748\ 5$ K), tin point (505.078 K), zinc point (692.677 K), aluminum point (933.473 K) and the silver point (1 234.93 K) by radiance comparison against the copper point, with a set of radiation thermometers having center wavelengths ranging from 0.65 μm to 1.6 μm. The copper-point temperature was measured by the absolute radiation thermometer which was calibrated by radiance method traceable to the electrical substitution cryogenic radiometer. The radiance of the fixed-point blackbodies was measured by standard radiation thermometers whose spectral responsivity and nonlinearity are precisely evaluated, and then the thermodynamic temperatures were determined from radiance ratios to the copper point. The values of $T - T_{90}$ for the silver-, aluminum-, zinc-, tin- and indium-point cells were determined as −4 mK ($U = 104$ mK, $k = 2$), −99 mK (88 mK), −76 mK (76 mK), −68 mK (163 mK) and −42 mK (279 mK), respectively.

Keywords Fixed point · Radiation thermometry · Thermodynamic temperature

Selected Papers of the 13th International Symposium on Temperature, Humidity, Moisture and Thermal Measurements in Industry and Science.

✉ Y. Yamaguchi
yamaguchi-yu@aist.go.jp

[1] National Metrology Institute of Japan, AIST, 1-1-1 Umezono, Tsukuba, Ibaraki 305-8563, Japan

1 Introduction

The International Temperature Scale of 1990 (ITS-90) has been in place for more than 25 years and has inherent weaknesses, including known discrepancies from thermodynamic temperature. In view of this, the Consultative Committee on Thermometry (CCT) of the International Committee for Weights and Measures (Comité International des Poids et Mesures, CIPM), at its 27th meeting in 2014, adopted a declaration encouraging National Metrology Institutes (NMIs) "to conduct significant experiments for the determination of thermodynamic temperature, to ensure that the SI unit kelvin is realized and disseminated in an optimum way in the coming decades" [1]. New thermodynamic temperature determinations are required to support the introduction and implementation of the *mise en pratique* for the definition of the kelvin (*MeP*-K), to facilitate direct dissemination of the redefined kelvin and to generate the background data required for a new unified temperature scale of improved thermodynamic consistency compared to the currently defined scales. The difference between thermodynamic temperature and ITS-90 ($T - T_{90}$) has been investigated with primary thermometry, such as the constant-volume gas thermometry, acoustic gas thermometry, dielectric-constant gas thermometry, noise thermometry and spectral radiation thermometry [2]. CCT regularly reviews all available measurement results and provides consensus estimates of the $T - T_{90}$ [3,4].

In high temperature range, thermodynamic temperatures of several high-temperature fixed points (HTFPs) above the copper point were recently determined within a multinational project, the CCT HTFP Program [5]. The final work package of the project [WP5/simultaneously WP1 of the Implementing the new kelvin (InK) project of the European Metrology Research Program (EMRP)] involved measurement of phase transition temperatures of the fixed points by the participating NMIs' absolute radiation thermometry capabilities [6]. The National Metrology Institute of Japan (NMIJ) joined the project and reported values of the HTFPs measured with absolute radiation thermometry traceable to an electrical substitution cryogenic radiometer [7] and other participating institutes also adopted similar detector-based methods using optical standards and silicon detectors [8]. For example, thermodynamic temperature of the copper point was determined as 1 357.802 K with uncertainty of 81 mK ($k = 2$), which is consistent with previously estimated $T - T_{90}$ [3].

The next step will be to extend the method to below the copper point, such as the silver point ($T_{90} = 1\,234.93$ K), the aluminum point (933.473 K), the zinc point (692.677 K), the tin point (505.078 K) and the indium point (429.748 5 K), in order to contribute to the consensus estimates of the $T - T_{90}$. For thermodynamic temperature measurements of these lower-temperature fixed points, radiometers with infrared wavelength bands have been used to obtain sufficient sensitivity and signal-to-noise ratio [9,10]. However, it is not straightforward to achieve small uncertainty at these fixed points because the wavelength bands are out of the responsivity model of silicon trap detectors, which were used for the calibration of thermometers to measure the HTFPs.

On the other hand, relative spectral radiation thermometry that utilizes radiance comparison against a reference fixed point with a known thermodynamic temperature has been established as an effective way to measure thermodynamic temperature [11,

12]. In this paper, we adopt thermodynamic temperature determination with relative method traceable to a fixed-point cell whose thermodynamic temperature has been predetermined precisely: Measurements were taken for five fixed-point blackbody cells from the silver point to the indium point by radiance comparison at several wavelengths, by measurement traceable to the copper-point cells of the CCT HTFP Program WP5/EMRP InK project WP1.

2 Measurement Scheme to the Indium Point

Spectral radiance of a blackbody is described by the Planck's law,

$$L(\lambda, T) = \frac{2hc^2}{n^2\lambda^5} \cdot \frac{1}{\exp(hc/kn\lambda T) - 1}, \tag{1}$$

where L, λ, h, c, n and k are the spectral radiance, wavelength, Planck constant, speed of light, index of refraction of the medium and Boltzmann constant, respectively. Relative spectral radiation thermometry gives blackbody temperature from the spectral radiance ratio to a blackbody of a known temperature.

Thermodynamic temperatures of fixed-point blackbodies below the copper point were determined with radiance comparisons as follows: First, two reference copper-point cells (Cell Band D of the HTFP Program/InK project) and an NMIJ copper-point cell were measured with the radiation thermometer with center wavelength of 0.79 μm and the difference of the NMIJ cell from the two reference cells was obtained. The thermodynamic temperature of the NMIJ cell was calculated from the thermodynamic temperatures of the reference cells assigned in [6] as a consensus estimate of measurements conducted by nine participating NMIs. Then, by radiance comparison to the NMIJ copper point at wavelengths of 0.65 μm and 0.79 μm, temperature of a silver point blackbody cell was determined. In a similar way, aluminum and zinc points were measured with the silver point serving as a reference at wavelengths of 0.9 μm and 1.0 μm. Finally, relative spectral responsivity of a radiation thermometer with center wavelength of 1.6 μm was characterized using radiance of the silver, aluminum and zinc points and applying the Sakuma–Hattori equation,

$$S(T) = \frac{C}{\exp(c_2/(AT + B)) - 1}, \tag{2}$$

where S is a signal of the radiation thermometer, c_2 is the second radiation constant and the coefficient A, B, and C are the parameters of the spectral responsivity determined by the fit. This approach has been applied in the past to measure the thermodynamic temperatures of the copper point and T_{90} of the Co-C eutectic point [12,13]. In the current investigation, extrapolation of the function is made in the opposite direction, i.e., to lower temperature, and thermodynamic temperatures of tin and indium points were determined (Fig. 1).

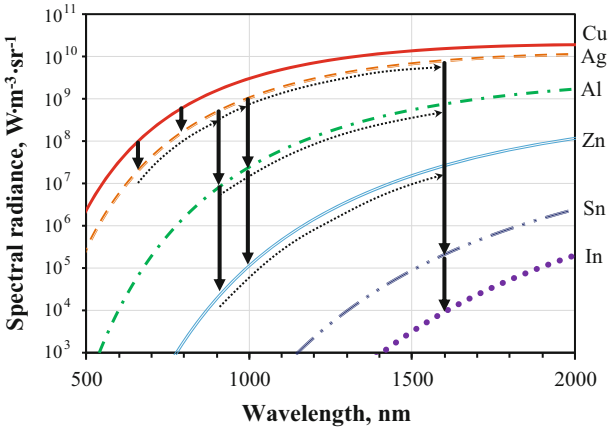

Fig. 1 Measurement scheme of radiance comparison down to the indium point

Fig. 2 Arrangement of the fixed-point sources and the radiation thermometers within the laboratory

3 Facilities

The fixed-point and standard radiation thermometer facilities at the NMIJ have unified designs: The six fixed-point blackbody units of the same cell design were installed in the same type blackbody furnaces, and standard radiation thermometers of the same series with four different wavelengths were employed in the measurements, which are well characterized and managed within the calibration system (Fig. 2). Therefore, emissivity, furnace effect, size-of-source effect (SSE) and other uncertainty factors involved in the comparison measurement could be minimized.

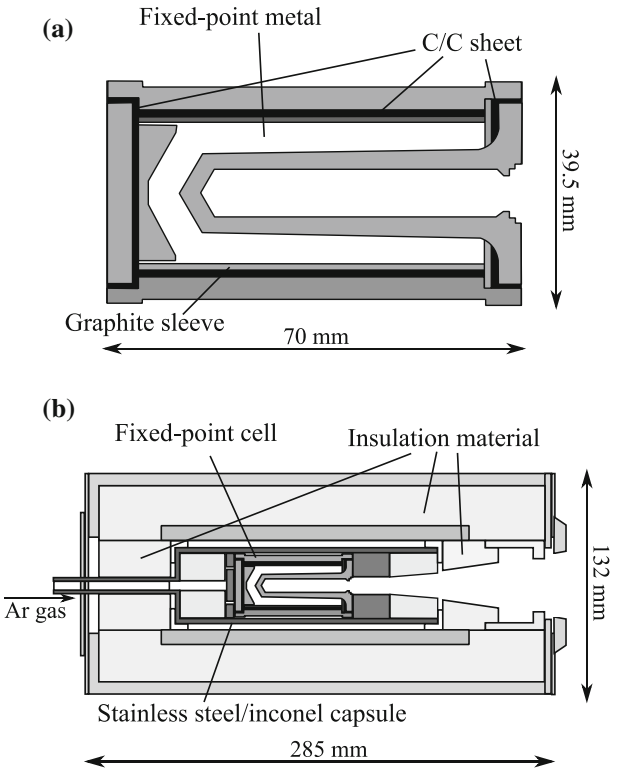

Fig. 3 Schematic diagram of the NMIJ standard blackbody furnace. (a) Fixed-point blackbody cell and (b) cell unit and blackbody furnace

3.1 Fixed-Point Blackbody

The fixed-point blackbodies consist of units of the same design that can be installed in the same type blackbody furnace (Chino IR-R0A) [14]. The blackbody cavity at the front of the cell has length and diameter of 52 mm and 8 mm, respectively (Fig. 3a). The base is a cone shape of 120°, and graphite interchangeable apertures with diameters of 3 mm or 6 mm are installed in front of the cavities. The emissivity is estimated as 0.999 87 for the 3 mm aperture and 0.999 47 for the 6 mm aperture assuming graphite emissivity of 0.85 (Table 1). For Cu, Ag, Al and Zn fixed points, the metal ingot is provided from the supplier (JX Nippon Mining & Metals) in one piece preformed in the shape to fit the crucible maintaining its 99.999 9 % purity.

Figure 3b shows the structure of the blackbody cell unit and furnace. Each fixed point is an individual unit and the same furnace can be switched easily from realizing one fixed-point type to another by replacing the fixed-point unit. The unit consists of sacrificial graphite pieces to protect the crucible from ambient air and contaminants in the purge gas, insulation materials and Inconel or stainless steel tube. The furnace is equipped with a heater surrounding the unit, whose temperature is monitored by a thermocouple and PID controlled by a digital controller. Freezing/melting plateaux are

Table 1 Fixed-point cells for the radiance comparisons

	S/N	Metal shape	Purity	Aperture/mm	Emissivity
Cu	CuC05	Ingot	6N	$\phi 3$	0.999 87
Ag	AgC03	Ingot	6N	$\phi 6$	0.999 47
Al	AlC04	Ingot	6N	$\phi 6$	0.999 47
Zn	ZnC04	Ingot	6N	$\phi 6$	0.999 47
Sn	SnC01	Shot	6N	$\phi 6$	0.999 47
In	InC01	Shot	6N	$\phi 6$	0.999 47

realized with the temperature setting of ± 20 K relative to the fixed-point temperature, and their durations are around 15 min.

3.2 Radiation Thermometers

The radiances of the fixed-point cells were measured with two types of radiation thermometers, Linear Pyrometer 5 (LP5, IKE) and IR-RST (Chino) (Table 2).

The spectral responsivity of the LP5 was evaluated based on radiance method, in which a radiation thermometer is calibrated as a filter radiometer by absolute radiometry [15], with a supercontinuum-source-based monochromator facility [7]. The monochromator output was introduced into an integrating sphere to act as an extended monochromatic source, and the thermometer responsivity was compared with that of a silicon trap detector that is traceable to the cryogenic radiometer of Physikalisch-Technische Bundesanstalt (PTB). The monochromator wavelength was precisely measured by a spectral analyzer. Other thermometer characteristics such as nonlinearity, SSE and gain ratio were also evaluated.

The IR-RST thermometers have similar optical systems carrying a silicon or an InGaAs detector, with center wavelengths of 0.65 μm, 0.9 μm, 1.0 μm and 1.6 μm [16] (Fig. 4). The wavelength of use is chosen according to measuring temperature ranges. The target diameters are narrowed to 1 mm for 0.65 μm, 4 mm for 0.9 μm, 1.0 μm, and 1.6 μm instruments by the field stop, at the measurement distance of 700 mm. Spectral responsivities, except for the 1.6 μm radiation thermometer, were measured to signal levels of around 10^{-6} from the peak with a double-monochromator system. The nonlinearity, SSE and gain ratio were also characterized for each thermometer.

4 Results and Discussion

4.1 $T - T_{90}$ of the Fixed Points

Representative freezing plateaux of the NMIJ standard cells are shown in Fig. 5, where emissivity, nonlinearity, SSE and gain ratio are corrected for. The temperature of each plateau was determined by taking the average of the middle half of the plateau, whose start and end points were determined as the intersection with the threshold level 0.05

Table 2 Radiation thermometers for the radiance comparisons

Model	S/N	Detector	Calibration method	Center wavelength/μm	Bandwidth/nm	Temperature range/°C	Target size/mm	Nonlinearity/%	SSE/%
LP5/IKE	8065	Si	Absolute	0.79	25	700 to 2 800	ϕ1	<0.001	<0.01
IR-RST/Chino	132A001	Si	Relative	0.65	12	960 to 3 000	ϕ1	<0.001	<0.03
IR-RST/Chino	142A002	Si	Relative	0.9	70	400 to 2 000	ϕ4	<0.002	<0.04
IR-RST/Chino	119A001	Si	Relative	1.0	83	400 to 1 100	ϕ4	<0.004	<0.05
IR-RST/Chino	133A001	InGaAs	Interpolation	1.6	142	150 to 960	ϕ4	<0.002	<0.08

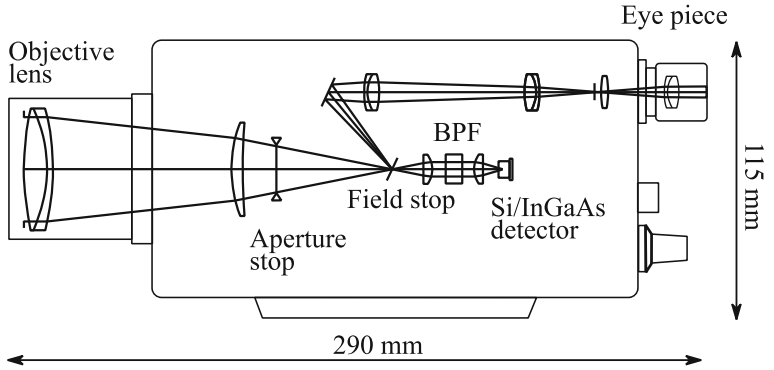

Fig. 4 Schematic diagram of the NMIJ standard radiation thermometer

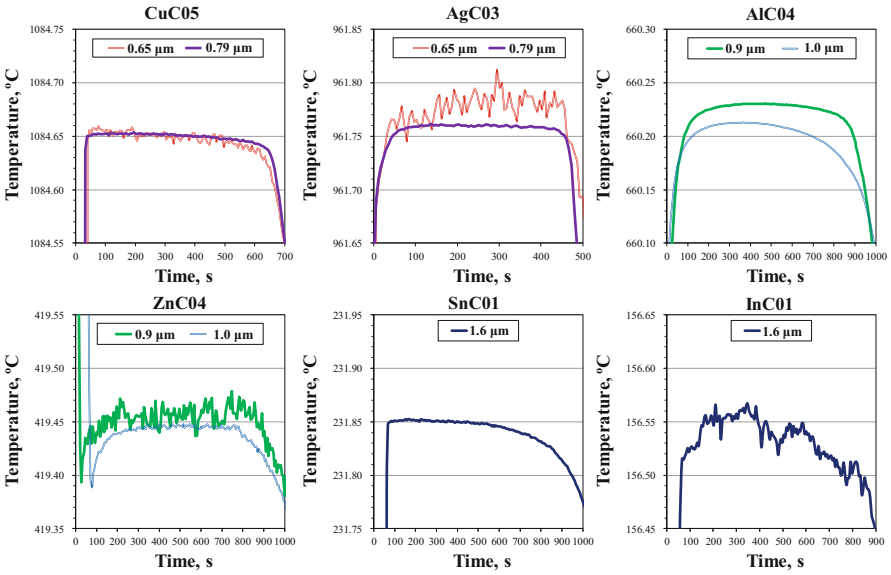

Fig. 5 Example of freezing plateaus of the fixed-point cells

K below the maximum value. Combinations of fixed points and thermometer wavelengths are listed in measurement time sequence in Table 3, along with the obtained values for the thermodynamic temperature of the measurement cells. For each measurement, three plateaux of the reference cell and of the measuring cell were measured alternately within a single day.

By taking the difference between the thermodynamic temperature, determined with reference to that of the reference cells and corrected for drift of the radiation thermometer, and the defined temperature of ITS-90, the $T - T_{90}$ of the NMIJ copper-point cell (CuC05) was determined as +35 mK. The $T - T_{90}$value of the silver point cell is calculated as −4 mK from the weighted mean of the radiance comparison result at 0.65 µm and 0.79 µm. In a similar way, from the measurements at 0.9 µm and 1.0 µm,

Table 3 Measurement combination and results of the radiance comparisons

Date	Wavelength/μm	Reference cell	Measurement cell	Thermodynamic temperature/K
25 March 2015	0.79	–	CuC05	1 357.821
10 April 2015	0.79	–	InK Cu/B	1 357.800[a]
13 April 2015	0.79	–	InK Cu/D	1 357.807[a]
17 April 2015	0.79	–	CuC05	1 357.808
10 June 2015	0.79	CuC05	AgC03	1 234.914
15 June 2015	0.65	CuC05	AgC03	1 234.938
25 June 2015	0.9	AgC03	AlC04	933.384
26 June 2015	0.9	AgC03	ZnC04	692.603
6 July 2015	1.0	AgC03	ZnC04	692.599
7 July 2015	1.0	AgC03	AlC04	933.364
28 July 2015	1.6	AgC03/AlC04	[b]	–
29 July 2015	1.6	AgC03/ZnC04	[b]	–
27 July 2015	1.6	AgC03	SnC01	505.010
5 August 2015	1.6	AgC03	InC01	429.707

[a] Thermodynamic temperature from [6]
[b] Measurement for spectral characterization

$T - T_{90}$ of the aluminum- and zinc-point cells were determined as −99 mK and −76 mK, respectively. Then, for the tin and indium points, $T - T_{90}$ was evaluated as −68 mK and −42 mK with the 1.6 μm radiation thermometer (Fig. 6).

4.2 Uncertainty

The uncertainty budget table for the determination of the thermodynamic temperature of the NMIJ fixed points is shown in Table 4. Except for the last line, the values are the relative uncertainty in the radiance. The uncertainty of the reference copper-point cells is the combined value of the uncertainties in the thermodynamic temperature assignment and the temperature deviation of each cell [6]. The uncertainties in the fixed-point measurements include plateau widths, repeatability, noise and dark-current drift. The InK copper cells were operated in a different type of furnace, so SSE correction was applied to the copper-point measurement, whereas SSE can be ignored in the comparison measurements of the silver point and below. On the other hand, the uncertainties due to spectral responsivity and nonlinearity are considered on the comparisons of cells with different radiance levels. The uncertainty due to spectral responsivity of the 1.6 μm radiation thermometer is calculated by the Monte Carlo method taking into account correlation among the reference fixed points, in which the uncertainty of the all reference temperatures is taken into account. The uncertainty of reference temperature is inversely proportional to the wavelength. Whereas the major component at the copper, silver and aluminum points is the reference value, the uncertainty due to spectral responsivity is dominant at the zinc point and below. In

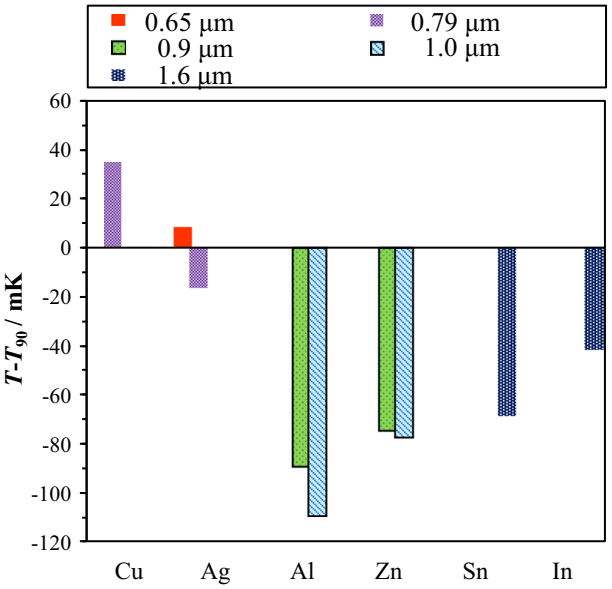

Fig. 6 Differences between measured thermodynamic temperature and the temperature defined in the ITS-90

addition, at the indium point, the uncertainty due to fixed-point measurement reaches major level owing to noise and limited stability of the 1.6 µm radiation thermometer.

4.3 Discussion

The summary of thermodynamic temperatures and expanded uncertainties of the fixed points is shown in Fig. 7. The $T - T_{90}$ values of the fixed points below the copper point are negative and are not consistent with the estimated values [3] within the uncertainty at the aluminum and zinc points. Because the measured fixed-point cells and the radiation thermometers have been group-managed, it is unlikely that the disagreements are caused by individual equipments. In prior researches using radiance comparison, the temperature interval between the Cu point and the fixed points below it also tended to be larger than expected. For example, $T - T_{90}$ value of the Cu point was reported to be +70 mK [12] determined with a radiation thermometer calibrated at In, Sn, Zn, Al and Ag points, whose temperatures were corrected with estimated $T - T_{90}$ values in [3]. The silver–copper temperature interval in terms of ITS-90 was reported to be 122.89 K and 122.87 K by NPL and LNE-Cnam, respectively [17], whereas that in the definition of the ITS-90 is 122.84 K. However, the disagreements with the estimated $T - T_{90}$ in Fig. 7 found in the current investigation are larger than these. We envisage to conduct further investigation in to the possible common cause, such as oxidation of fixed-point metals or thermometer spectral responsivity characterization.

Table 4 Uncertainties of temperature for the fixed-point cells

Component	Uncertainty/10^{-4}					
	Cu	Ag	Al	Zn	Sn	In
Reference cell						
Reference temperature	5.0	5.5	4.9	4.9	3.1	3.1
Emissivity	1.2	1.0	2.0	2.0	2.0	2.0
Fixed-point measurement	0.3	0.3	0.0	0.0	0.1	0.1
Measurement cell						
Emissivity	1.0	2.0	2.0	2.0	2.0	2.0
Fixed-point measurement	0.2	0.3	0.4	1.9	8.0	44
Comparison						
Spectral responsivity	–	1.9	3.8	9.2	27.2	51
SSE	0.1	–	–	–	–	–
Nonlinearity	–	0.0	2.3	3.0	2.1	0.6
Drift	1.5	–	–	–	–	–
Combined standard uncertainty	5.5	6.2	7.2	11.4	28.8	67.7
Expanded uncertainty ($k = 2$)	10.9	12.4	14.5	22.8	57.6	135
	Uncertainty/K					
Expanded temperature uncertainty ($k = 2$)/K	0.111	0.104	0.088	0.076	0.163	0.279

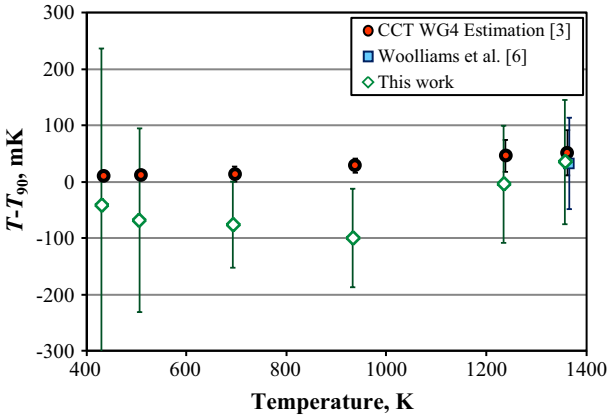

Fig. 7 Measured $T - T_{90}$ of the fixed points

5 Conclusion

Thermodynamic temperatures of the silver, aluminum, zinc, tin and indium points were measured by radiance comparison method with reference to the consensus estimate value of the copper-point measurement in the CCT HTFP Program. The $T - T_{90}$ of the NMIJ copper-point cell was determined as +35 mK. The radiance of the fixed-point blackbodies was measured by the standard radiation thermometers with center wavelengths ranging from 0.65 μm to 1.6 μm. The values of $T - T_{90}$ for the silver, aluminum, zinc, tin and indium points cells were determined as −4 mK ($U = 104$ mK, $k = 2$), −99 mK (88 mK), −76 mK (76 mK), −68 mK (163 mK) and −42 mK (279 mK), respectively, which are lower than the previously estimated $T - T_{90}$.

References

1. CCT, *CCT/SUMM-DE2014*. http://www.bipm.org/cc/AllowedDocuments.jsp?cc=CCT. Accessed July 2016
2. J. Fischer, B. Fellmuth, Rep. Prog. Phys. **68**, 1043–1094 (2005)
3. CCT WG4, *Estimates of the differences between thermodynamic temperature and the ITS-90*. http://www.bipm.org/utils/common/pdf/ITS-90/Estimates_Differences_T-T90_2010.pdf. Accessed July 2016
4. J. Fischer, M. de Podesta, K.D. Hill, M. Moldover, L. Pitre, R. Rusby, P. Steur, O. Tamura, R. White, L. Wolber, Int. J. Thermophys. **32**, 12–25 (2011)
5. G. Machin, P. Bloembergen, J. Hartmann, M. Sadli, Y. Yamada, Int. J. Thermophys. **28**, 1976–1982 (2007)
6. E.R. Woolliams, K. Anhalt, M. Ballico, P. Bloembergen, F. Bourson, S. Briaudeau, J. Campos, M.G. Cox, D. del Campo, W. Dong, M.R. Dury, V. Gavrilov, I. Grigoryeva, M.L. Hernanz, F. Jahan, B. Khlevnoy, V. Khromchenko, D.H. Lowe, X. Lu, G. Machin, J.M. Mantilla, M.J. Martin, H.C. McEvoy, B. Rougié, M. Sadli, S.G.R. Salim, N. Sasajima, D.R. Taubert, A.D.W. Todd, R. Van den Bossche, E. van der Ham, T. Wang, A. Whittam, B. Wilthan, D.J. Woods, J.T. Woodward, Y. Yamada, Y. Yamaguchi, H.W. Yoon, Z. Yuan, Phil. Trans. R. Soc. A **374**, 1–22 (2016)
7. Y. Yamaguchi, Y. Yamada, J. Ishii, Int. J. Thermophys. **36**, 1825–1833 (2015)
8. K. Anhalt, G. Machin, Philos. Trans. R. Soc. A **374**, 1–17 (2016)
9. G.P. Epeldauer, H.W. Yoon, J. Zeng, T.C. Larason, Int. J. Thermophys. **32**, 2197–2205 (2011)
10. N. Noulkow, R.D. Taubert, P. Meindl, J. Hollandt, Int. J. Thermophys. **30**, 131–143 (2009)
11. J. Fischer, H.J. Jung, Metrologia **26**, 245 (1989)
12. M. Battuello, M. Florio, F. Girard, Metrologia **47**, 231–238 (2010)
13. M. Battuello, F. Girard, M. Florio, Metrologia **46**, 26–32 (2009)
14. F. Sakuma, L. Ma, T. Suzuki, T. Kobayashi, A. Nakanishi, H. Katayama, *Proceedings of SICE 2004*, FPI-4-2, pp. 72–76 (2004)
15. H.W. Yoon, C.E. Gison, G.P. Eppeldauer, A.W. Smithm, S.W. Brown, K.R. Lykke, *Opt. Radiat. Meas. Based Detect. Stand.*, **29**, 239 (2009)
16. F. Sakuma, L. Ma, T. Kobayashi, Int. J. Thermophys. **29**, 312–321 (2008)
17. H.C. McEvoy, M. Sadli, F. Bourson, S. Briaudeau, B. Rougié, Metrologia **50**, 559–571 (2013)